Annual Conference of the PHM Society, Volume 3, Issue 1, September 2011
DOI: 10.36001/phmconf.2011.v3i1.2033

Defect source location of a natural defect on a high speed-rolling element bearing with Acoustic Emission

B Eftekharnejad[1], A. Addali[2] and D Mba[2]

[1] Renewable Energy Systems Ltd, Kings Langley, WD4 8LR United Kingdom
[2] School of Engineering, Cranfield University, Bedford, England, MK43 0AL
Email: A.Addali@cranfield.ac.uk

Abstract
The application of Acoustic Emission (AE) technology for machine health monitoring is gaining ground as powerful tool for health diagnosis of rolling element bearings. The successful application of AE to life prognosis of bearings is very dependent on the ability of the technology to identify and locate a defect at its earliest stage. Determining source locations of AE signals originating in real time from materials under load is one of the major advantages of the technology. This paper presents results which highlight the ability of AE to locate naturally initiated defects on high-speed roller element bearing in-situ. To date such location has only be successfully demonstrated at rotational speeds of less than 100 rpm.

1. Introduction

The rolling element bearing is the most common part of rotating machines. The continued interest in condition-based maintenance of industrial assets has lead to a growing interest in monitoring of rolling bearings. The application of Acoustic Emission (AE) in monitoring the rolling element bearings has grown in popularity over the past few decades [1]. To date most of the published work has studied the applicability of AE technology in detecting seeded faults artificially introduced on the bearing. Yoshioka [2] was one of the earliest researchers who studied the applicability of AE in detecting naturally degraded bearings. Later, Elforjani et al [3] conducted an experiment aimed at building on Yoshioka's work. Their results showed the effectiveness of AE in detecting the onset of bearing failure, identifying the circumferential location of the defect on the race at very early stages of degradation, and the diagnostic potential of enveloping AE signatures. Although conclusive, this research was not representative of the broad operation range of bearings as the test was undertaken at a slow rotational speed (72 rpm). The results presented in this paper aims to complement the work of Elforjani [3, 4] by experimentally investigating the use of AE for detecting and locating the natural pitting of a bearing rotating at 1500 rpm in which significantly higher background AE operating noise is expected.

2. Experimental Setup

The test rig used in this experiment is displayed in **Figure 1**. The bearing test rig has been designed to simulate varying operating conditions and accelerate natural degradation. The chosen bearing for this study was an SKF single thrust ball bearing, model number SKF51210. To ensure accelerated failure of the race the standard grooved race was replaced with a flat race, model number SKF 81210TN. This caused a point contact between the ball elements and the race resulting in faster degradation of the race and early initiation of sub-surface fatigue cracks. The

load on the test bearing was applied by a hand operated hydraulic pump (Hi-Force No: HP110-Hand pump-Single speed-Working Pressure: 700 BAR). The flat race was fitted onto the loading shaft in a specifically designed housing. This housing was constructed to allow for placement of AE sensors directly onto the race. Modifications were made to the support of the flat bearing race so as to allow positioning of the AE sensors, see Figure 2. The placement of the AE sensors was such that it facilitated the identification of the source of AE during operation. The motor on the rig operated at 1500rpm and the number of rolling element in the test bearing was 14 and the ball pass frequency (BPF) was 175Hz.

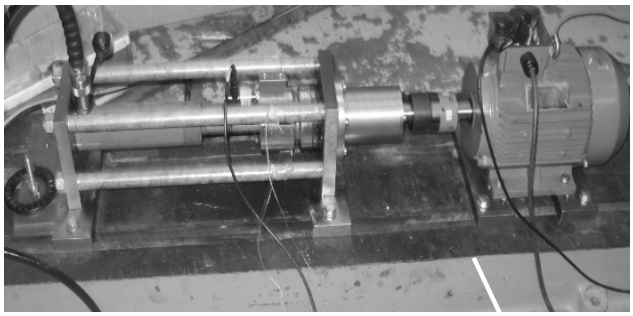

Figure 1 Test rig assembly

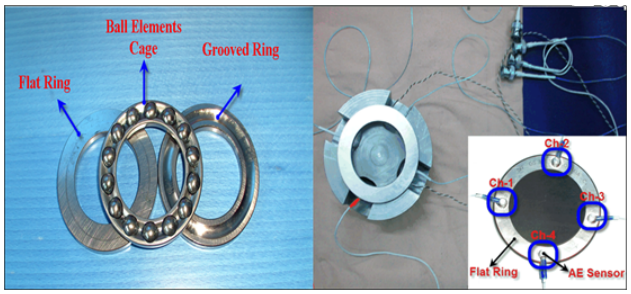

Figure 2 Test bearing and sensor arrangement on the flat race.

The AE acquisition system employed commercially available piezoelectric sensors (Physical Acoustic Corporation type 'PICO') with an operating range of 200–750 kHz at temperatures ranging from 265 to 1770C. The AE sensors were connected to a data acquisition system through a preamplifier (40dB gain). The system was set to continuously acquire AE absolute energy (atto-Joules) over a time constant of 10 ms at a sampling rate of 100 Hz. The absolute energy is a measure of the true energy and is derived from the integral of the squared voltage signal divided by the reference resistance (10 k-Ohms) over the duration of the AE signal. For these tests a fixed sample length (250msec) of AE waveforms were captured every 60 seconds at 2 MHz sampling frequency. Throughout the test AE HITs were also acquired. An Acoustic Emission HIT is normally described by several parameters such as threshold, duration, counts and rise time. The AE signal duration is the time between the first and last amplitude threshold crossing while the rise time is the time between the start of the HIT and the instant at which the maximum amplitude of HIT is reached, see figure 3. Also, a single AE event can be produced by number of AE HITs. In addition to this, the timing parameters employed for defining an event during these experiments included the HIT definition time (HDT), HIT lockout time (HLT) and peak definition time (PDT) and these were set at 500 µsec, 500 µsec and 100 µsec respectively. Correctly setting the PDT will result in an accurate measurement of peak amplitude while the appropriate definition of HDT will ensure that each signal generated from the structure is reported as one HIT. As it defines the period over which a HIT can be acquired. With an accurate setting of HLT spurious measurement during the signal decay will be avoided [5]; essentially it defines the period between successive HITs; its second function is to inhabit the measurement of reflections .In addition, an accelerometer (ISO BASE Endevco 236 with repose between 10 and 8000 Hz) was mounted on the flat race housing and vibration measurements were acquired at sampling of 10 kHz at three-minute intervals using a NI-6009 USB analog to digital data acquisition card.

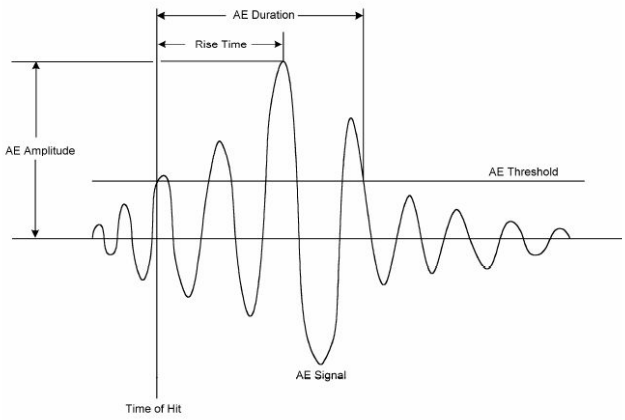

Figure 3 Schematic representation of an AE Hit [5]

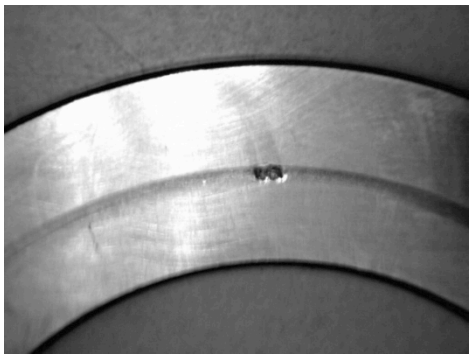

Figure 4 Defect on the outer race at termination of bearing test

3. Test procedure

For the purpose of this experiment the following procedure was undertaken to determine the subsurface stresses on the test bearing and thereby estimate the time, or number of cycles, prior to a surface defect on a track. Theories employed for this procedure, particularly for the flat race, included the Hertzian theory for determining surface stresses and deformations, the Thomas and Hoersh theory for subsurface stress, and the Lundberg and Palmgren theory for fatigue evaluation. For the grooved race the standard procedure, as described by BS 5512,1991, was employed for determining dynamic load rating. The theoretically determined life was calculated to be approximately 16 hours though the actual test duration was significantly longer. The test rig was allowed to operate until a spall was induced on the flat race and figure 4 shows the developed defect upon the termination of the tests. At this time abnormal vibration levels were registered and the rig was stopped. A load of approximately 50000N was applied on the bearing throughout the test. The test was stopped at 278 minutes though the AE measurement failed after 220 min due to excessive temperatures experienced on the bond holding the sensor to the race.

4. Results and Discussion

4.1 Real time monitoring of the Vibration and AE levels

The overall trends of Acoustic Emission activity and the vibration r.m.s noted for the duration of both tests are presented in Figure 5. There was an initial rise in AE and vibration levels at the very start of the tests. This is associated with the run-in period. After this period both vibration and AE levels remained level for approximately 40mins after which a noticeable increase in AE was again observed from 40mins of operation though vibration levels remained constant. The drop in vibration levels at 50mins into operation was due to a glitch in the vibration recording system that was fixed immediately. Comparing the overall trend of vibration and AE r.m.s it is evident that the AE is more sensitive in monitoring the progression of the defect. This was because the AE level began to increase continuously much earlier than vibration levels. It must be noted that these are accelerated failure tests and the difference in time between these techniques (AE and vibration) in identification of the defect will most certainly be much longer for non-accelerated test conditions; further highlighting the increased sensitivity of the AE technology.

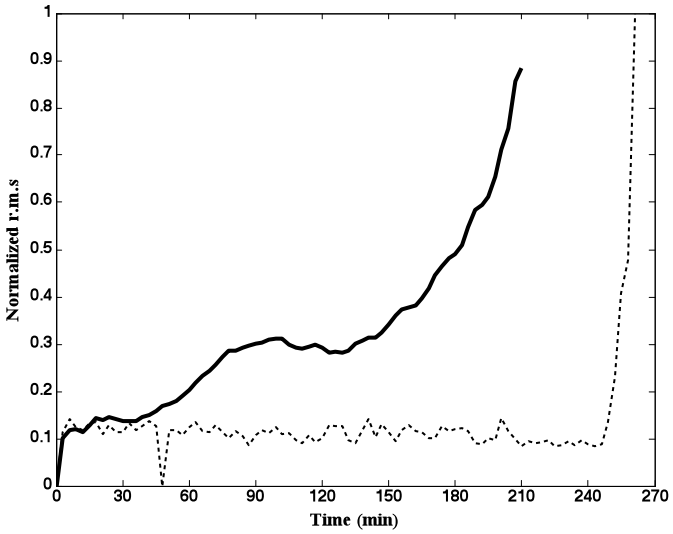

Figure 5 Overall AE (--) and vibration (….) r.m.s levels

The AE and vibration waveforms upon the termination of the test are presented in Figure 6. Evident were AE burst spaced at 175 Hz that corresponds to the bearing defect frequency, though not evident on the vibration plot. Also values of Kurtosis and Crest Factor [1] (CF) associated with AE signal are significantly higher than corresponding levels of vibration (Crest factor and Kurtosis values of 13 and 14.2 respectively for AE, and, 0.2 and 2.6 respectively for vibration), see Figure 6. This reiterates the diagnostic advantage of AE over vibration; as it is more sensitive to damage detection [1]. A time-frequency plot of a section of AE wave associated with a surface defect showed a broad frequency range (100 to 600 kHz), see figure 7.This shows the significant high frequency content of AE associated with the bearing defect. A Gabor wavelet transform on was employed to determine the time-frequency spectrum. For the wavelet analysis *AGU-Vallen Wavelet* software, developed by Vallen System GmbH, was employed [6]. Given this well-established view that AE is more sensitive than vibration, the aim of this paper in not to re-iterate the obvious but to assess the applicability of AE to locate the position of the growing defect in-situ on a high speed bearing in comparison to slow speed bearing tests that have already shown defect location with AE.

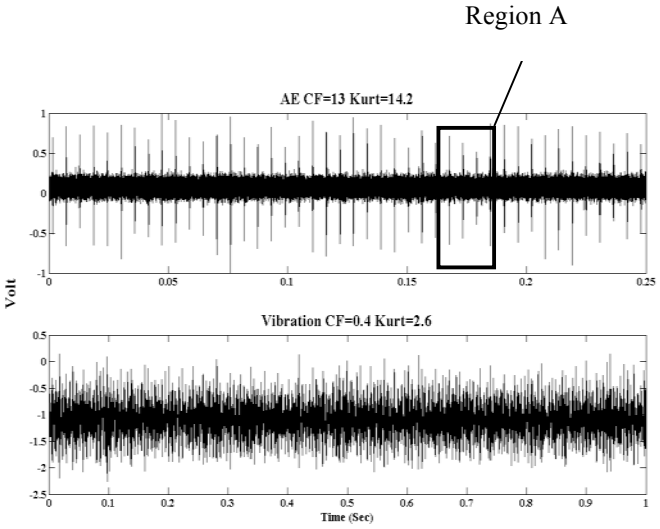

Figure 6 Acoustic Emission and vibration waveforms associated with the damaged bearing

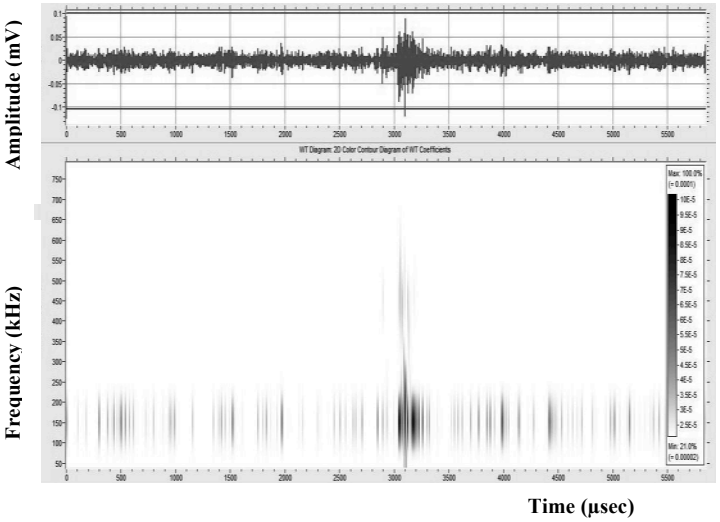

Figure 7 Time-frequency plot associated with a single AE burst from region A of Figure 6

4.2 Defect source location

The most common method for source location involves employing differences in time of arrival of waves at the receiving sensor. Given the actual

[1] *The CF defined as the ratio of the peak value divided by the signal r.m.s.*

location of the AE sensor and the wave velocity for the bearing material, the location of the AE source can be determined. The sensor positions on the race allow linear location of the source to be calculated which involves linear interpolation between the coordinates of two adjacent sensors based on the differences in arrival time at the receiving sensors. Simulated AE sources on the test bearing race (Hsu-Nelson) showed the dominant frequency content of AE's recorded to be approximately 300 kHz which corresponds to a velocity of 4000 m/s for the symmetric zeroth lamb wave mode (S_o) on steel at 1.8 mm MHz (0.3 MHz, and 6 mm thick race). This velocity was used for all source location investigations and prior to the onset of testing several Hsu–Nielsen sources were made at various positions on the surface to establish the accuracy at this velocity and specific threshold level. Results were within 4% of the exact geometric location of the Hsu–Nielsen sources. For this investigation, a threshold of 70 dB was set and whenever the threshold was exceeded, the location of the source is computed and identified. Further, any AE event detected above this threshold is assigned to the geometric position (source); this is a cumulative process and as such a fixed source will have the largest contributory events in a cumulative plot.

Figure 8 presents such a cumulative plot detailing location results for the test at three chosen operating times. The x-axis represents the circumferential distance between each sensor; the position of each sensor is detailed on each of the plots in figure 8. The y-axis of figure 8 details the number of AE events captured during the test. Observations showed that at 120mins and 180mins into operation the recorded events suggested activity in the vicinity of sensor 4, however by 206mins into operation, a large number of AE events were registered between sensor-1 and -2 suggesting the development of surface damage. The location of this abnormally high concentration of AE events matched the location of damage upon the termination of test, see figure 4. The events noted earlier in the test are attributed to spurious AE activity. Interestingly, the identification of the defect location become evident from the cumulative plots at approximately 200 minutes into operation even though AE levels had seen rising from 60 minutes into the test. The inability to identify the location much earlier into the test, unlike observations at the lower rotational speeds [3,4,7], is attributed to the higher operating background noise that makes identification of AE HITs more difficult. A direct comparison of AE operating noise at 72 rpm and 1500 rpm was noted to be 52 dB and 70 dB respectively. Such high operational noise level (70dB) could make source location significantly more challenging than at low rotational speeds. To enhance the ability to identify the defect location earlier would require advanced noise cancellation techniques.

5. Conclusion

The applicability of AE for source location of bearing defect in-situ has been demonstrated. Threshold levels above operating background levels have been shown to be sufficiently suitable for differentiating AE time of arrival intervals. This conclusion has been derived based on results from tests on a few experiments. Whilst the probability of having four AE sensors placed on a bearing race is limited it can be employed as a quality control tool for bearing manufacturers or applied on bespoke critical bearings.

6. References

[1] Mba, D., and Rao, R. B. K. N., 2006, "Development of Acoustic Emission Technology for Condition Monitoring and Diagnosis of Rotating Machines: Bearings, Pumps, Gearboxes, Engines, and Rotating Structures," Shock and Vibration Digest, 38(1) pp. 3-16.

[2] T. Yoshioka, 1992, "Application of Acoustic Emission Technique to Detection of Rolling Bearing Failure," J. Soc. Tribologists Lubrication Eng, 49.

[3] Elforjani, M., and Mba, D., 2009, "Assessment of Natural Crack Initiation and its Propagation in Slow Speed Bearings," Nondestructive Testing and Evaluation, 24(3) pp. 261.
[4] Elforjani, M., and Mba, D. [2010], "Accelerated Natural Fault Diagnosis in Slow Speed Bearings with Acoustic Emission," Engineering Fracture Mechanics, .
[5] Physical Acoustic Co., Pci2-Based AE system user manual
[6] http://www.vallen.de/

[7] Elforjani, M., and Mba, D., 2008, "Observations and Location of Acoustic Emissions for a Naturally Degrading Rolling Element Thrust Bearing," Journal of Failure Analysis and Prevention, **8**(4) pp. 370-385.

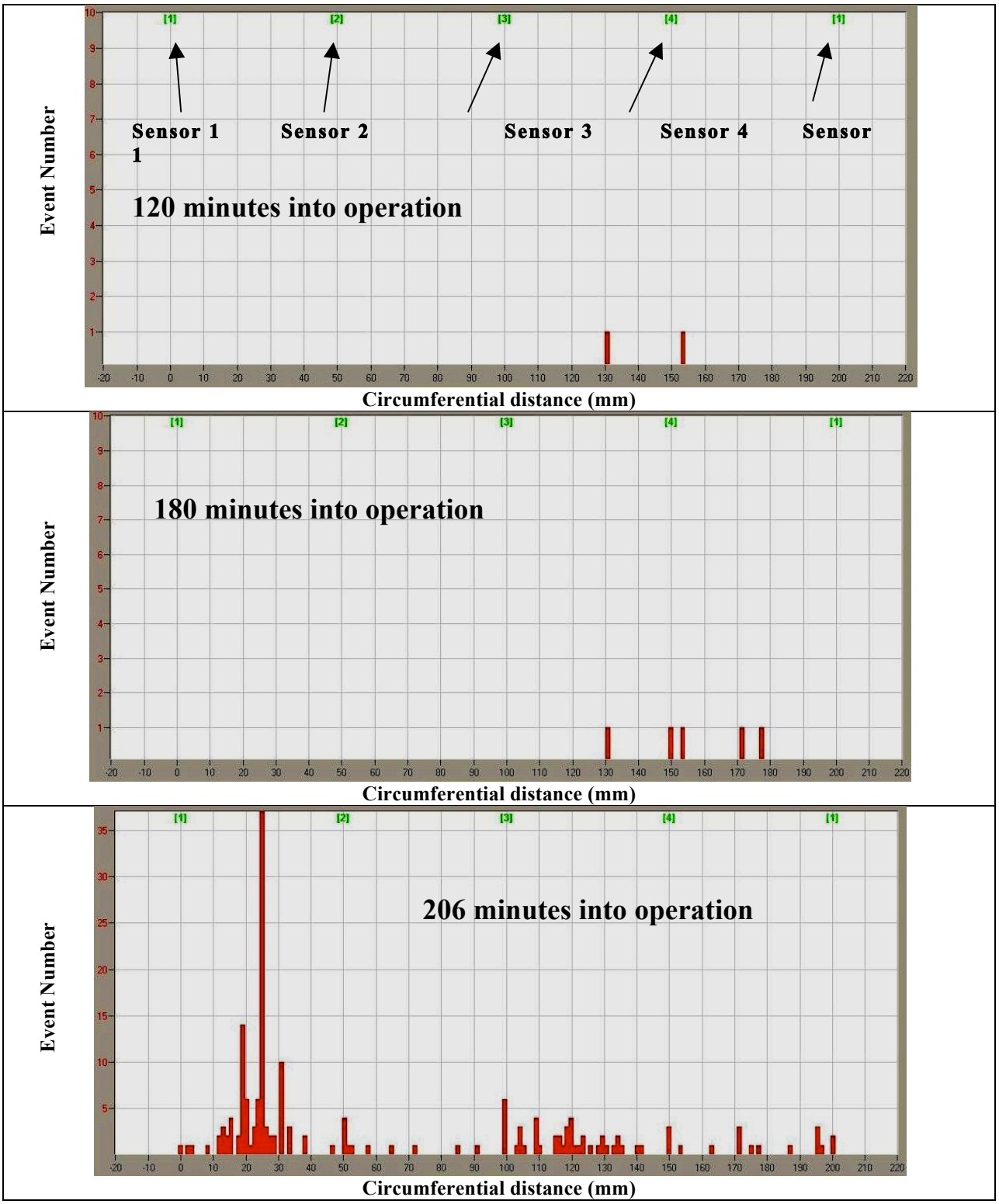

Figure 8 Acoustic Emission events against sensor position at different time intervals